Chalcogenide Letters Vol. 14, No. 3, March 2017, p. 79 - 85

SMALL ANGLE NEUTRON SCATTERING AND RAMAN MEASUREMENTS OF As-Se-S and As-Se-Te CHALCOGENIDE GLASSY SEMICONDUCTORS DOPED BY SAMARIUM

R.I. ALEKBEROV[a *], S.I. MEKHTIYEVA[a], A. I. ISAYEV[a],
M. FÁBIÁN[b,c], Q. TIAN[b] , L. ALMÁSY[b,d *]
[a]*G.M. Abdullayev Institute of Physics, Azerbaijan National Academy of Sciences AZ1143, Baku, G. Javid ave 131*
[b]*Wigner Research Centre for Physics, H-1525 Budapest P.O.B. 49, Hungary*
[c]*Centre for Energy Research, H-1525 Budapest P.O.B. 49, Hungary*
[d]*State Key Laboratory Cultivation Base for Nonmetal Composites and Functional Materials, Southwest University of Science and Technology, Mianyang, China*

In this work have been investigated the structural features of As-Se-S and As-Se-Te systems and their alloying with Sm on the nanometer scale using small-angle neutron scattering and Raman spectroscopy. These materials have two-phase porous structure, i.e. materials outfit with solid particles and includes free volumes. The parameters of fractal structure have been determined, in particular, the upper and lower boundaries of self-similarity and size of particles forming fractal clusters. The observed features of Raman scattering are associated with relaxation and excess density of states of acoustic vibrations in irregularities. Such irregularity areas are associated with the presence of nano-size inhomogeneities.

(Received December 9, 2016; Accepted March 1, 2017)

Keywords: Amorphous structure, chalcogenide glass, neutron scattering, Raman scattering

1. Introduction

Structure of amorphous and glassy semiconductors are generally characterised by local order in the arrangement of atoms inherent to crystalline bodies in their first coordination sphere, i.e. the presence of short-range order (SRO), and the lack of long range order (LRO), but also certain order in the arrangement of atoms and molecules exists in a region covering several coordination spheres, called usually medium-range order (MRO).

The microstructure of these materials depends on the regime of technological process, the chemical composition and alloying [1-7]. They also play a decisive role in the formation of relaxation and vibrational properties, and can be studied by various radiation scattering methods as well as by macroscopic properties measurements of electrical and thermal conductivity. A completely new approach to research on the influence to the wave processes of the structural features in disordered materials had appeared after the publication of articles about the relation of fractals and local vibrational states [8-9]. A recent trend is to describe the structure of amorphous materials by the fractal approach. In many materials, except homogeneous liquids or substances in the crystalline state, the scale invariance can be found in certain range of sizes, i.e. the components of the structural elements in nano-metric scale (clusters, the pores and the interface between them) have a fractal nature [10-12]. Since the change in the chemical composition and doping rare earth elements affects the structure of chalcogenide glassy semiconductors (CGS) at the middle order, it can be expected that changes occur also in the fractal characteristics of the structure, which is the topic of the present work.

As-Se-S and As-Se-Te CGS alloyed by samarium are important promising materials for optoelectronics [13-16]. In the present study we investigated the influence of chemical

*Corresponding authors: almasy@mail.kfki.hu

composition and doping with samarium in As-Se-S and As-Se-Te systems on the density, small-angle neutron scattering and Raman scattering.

2. Experimental

2.1. Sample preparation

Synthesis of CGS materials As-Se-S and As-Se-Te with Sm impurity was conducted in the following sequence: specially pure elementary substances in equal atomic percentages are filled into the quartz ampoules and after evacuating the air down to 10^{-4} mm Hg they were heated up to T = 900-950°C for 3 hours and kept for about 12 hours at this temperature. To maintain sample homogeneity the synthesis has been carried out in rotating furnace, while cooling has been carried out switching the furnace off. Sm impurities were introduced in synthesis process. The density of As-Se-S and As-Se-Te glass materials doped by Sm was measured by Archimedes' principle in water. The densities of chalcogenide glasses, ρ were calculated using the formula:

$$\rho = \left[\frac{w_0}{(w_0 - w_L)} \right] \rho_L \tag{1}$$

where w_0 and w_L are respectively the weight of material in air and in liquid (water) and ρ_L is the density of liquid (water) which is equal to 1 g.cm^{-3} at room temperature. The accuracy was better than ±0.02 g/cm^3.

2.2. Small-angle neutron scattering and Raman scattering experiments

Small-angle neutron scattering (SANS) measurements have been performed on the *Yellow Submarine* small-angle scattering instrument installed at the cold neutron beam line of the 10 MW steady-state research reactor of the Budapest Neutron Centre (BNC) Hungary [17]. The measurements were performed at room temperature. The films of 10 μm in thickness have been obtained by thermal evaporation with the rate 0.4-0.5 μm /min on the glass substrate in vacuum under the pressure 10^{-4} mm Hg. Raman scattering (RS) was measured on three-dimensional Confocal Lazer Microspectrograph (Tubitak, Turkey). The excitation has been carried out by 25 mWt He-Ne laser and wavelength 632.8 nm. Cross-section radius of the laser beam falling on the film was equal to 1 μm. System of Spectrograph Princeton Instruments Spec-10:400 V Digital CCD of system 7386-0001 with thermoelectric cooler served as a radiation detector. The detector was an Avalanche CCD OF camera CDD 1340×40 pix, 20×20 Mpix (26.8 mm×8.0mm). Exposure times were 90 sec.

3. Results and discussion

In Table 1. are collected the experimentally determined density values (ρ) for the investigated materials, while the density solid phase of material (ρ_0) is evaluated according to the tabulated density values of the individual components. As seen in the density of materials is less than the solid phase density, indicating the porous structure of the two-phase (solid-pore) of the materials, i.e. materials includes free volumes along with solid particles. Using these data, the fractional free volumes were estimated and presented in Table 1. Also in Table 1. are collected the experimental parameters determined from the small angle scattering measurements.

Table 1. The experimental density (ρ) of the samples and the density solid phase of material (ρ_0), Porod's index (n), fractal dimensions (D_S), the size of mono-disperse particles (r_0), Porod constant (K), the dimensions of the irregularities (d_{min}, d_{max}).

Samples	**n**	**D_S**	**d_{min}, nm**	**ρ (q/sm^3)**	**r_0, nm**	**K, cm^{-5}**	**Δρ, cm^{-2}**	**ρ_o (q/sm^3)**	**d_{max}, nm**	**ρ_o- ρ**	**ΔV/V (%)**
As_{40} Se_{60}	4.25	1.75	15.03	4.59	3.43	4.72×10^{26}	2.93×10^{9}	5.166	92.35	0.576	11.14
$As_{40}Se_{30}S_{30}$	4.19	1.81	14.37	2.879	3.34	1.29×10^{26}	1.51×10^{9}	4.35	92.35	1.471	33.81
$As_{33.3}$ $Se_{33.3}$ $S_{33.4}$	4.14	1.86	17.47	3.254	4.14	4.95×10^{25}	1.04×10^{9}	4.194	92.35	0.940	22.42
$As_{33.3}$ $Se_{33.3}$ $S_{33.4}$:$Sm_{2.5}$	4.68	1.32	23.94	3.123	5.57	2.43×10^{28}	2.68×10^{10}	4.382	92.35	1.259	28.73
$As_{33,3}$ $Se_{33.3}$ $S_{33.4}$ Sm_1	-	-	-	3.74	-	-	-	4.269	-	0.529	12.4
$As_{33.3}$ $Se_{33.3}$ $S_{33.4}$ Sm_5	-	-	-	4.07	-	-	-	4.570	-	0.500	10.95
$As_{33.3}$ $Se_{33.3}$ $Te_{33.4}$	4.12	1.88	14,37	5.768	3.43	6.3×10^{25}	1.07×10^{9}	5.587	92.35	0.180	3.2
As_{40} Se_{30} Te_{30}	4.25	1.75	19.58	5.132	4.62	4.51×10^{26}	3.32×10^{9}	5.601	92.35	0.469	8.37
$As_{33.3}$ $Se_{33.3}$ $Te_{33.4}$:$Sm_{2.5}$	3,85	2.15	13.19	4.84	3.05	2.47×10^{24}	1.99×10^{8}	5.775	92.35	0.935	16.19
$As_{33.3}$ $Se_{33.3}$ $Te_{33.4}$ Sm_1	-	-	-	4.95	-	-	-	5.662	-	0.712	12.58
$As_{33.3}$ $Se_{33.3}$ $Te_{33.4}$ Sm_5	-	-	-	3.60	-	-	-	5.963	-	2.363	39.63

As seen from Table 1., changes in chemical composition and doping have different effects on As-Se-S and As-Se-Te. Increase in the proportion of chalcogen (replacement $As_{40}Se_{30}S_{30}$ with $As_{33.3}Se_{33.3}S_{33.4}$) and samarium doping decreases the fractional free volume in As-Se-S. The fraction of free volume decreases at the excess chalcogen for As-Se-Te, and increases with alloying samarium of non-stoichiometric composition.

In Fig. 1 are presented the dependence of SANS intensity on the module of the scattering vector for samples of As-Se-S and As-Se-Te with different chemical composition, and also alloyed by Sm.

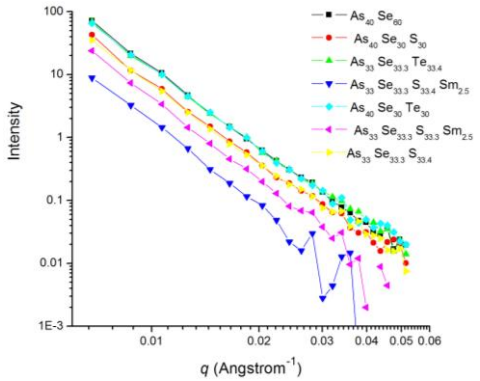

Fig. 1. SANS scattering data for the chalcogenide powder samples.

As seen from the graph, the intensity of scattered neutrons beginning from the value ~ 0.007 $Å^{-1}$ momentum transfer for all the samples obeys a power law $I(q) \sim q^{-n}$ and such dependence extends to values about 0.05 $Å^{-1}$ depending on the chemical composition. Such behavior of SANS scattering curves testifies the presence of a wide distribution of the scattering inhomogeneities in the area of size $R_{max} >> R_{min}$, when the conditions of [18].

$$R_{max}^{-1} << q << R_{min}^{-1} \quad (2)$$

Observation of power law also reveals that the size scale of the heterogeneity is large enough and satisfies condition $q_{min} \cdot R >> 1$. Bale et al. [19] suggested a practical criterion to determine the characteristic size of inhomogeneities: $q_{min} \cdot R \approx 3.5$. Using specified criteria in our materials the characteristic size of inhomogeneity has been obtained as R ≈ 515 Å. As seen from the table the values of the degree index determined from the slope of the dependence of SANS intensity on the modulus of the scattering vector built in double logarithmic scale changes as a result of variations in chemical composition and doping with samarium. For $As_{33.3}Se_{33.3}S_{33.4}$ and $As_{33.3}Se_{33.3}Te_{33.4}$ compositions values of index are n ≈ 4.12 ÷ 4.14, i.e. it can be argued that they obey the law of Porod.

$$I = \frac{2\pi\Delta\rho^2(S/V)}{q^4} = \frac{K}{q^4} \quad (3)$$

here Δρ is the difference in scattering length density between matrix and the object, which can be considered here as an open or closed empty void. S/V is the interfacial surface area per unit volume, therefore the scaling constant *K* is proportional to S/V. At the same time scattering objects are filling the three-dimensional space with sharp boundaries between the solid phase and pores, i.e. on this size scale the scattering from the interfaces is dominant and the possible fractal nature of the packing is not observed. As seen from Figure 1, the dependence of the SANS intensity from the scattering vector modulus, the transition to the Guinier region is not yet reached at the smallest measured *q*. From these data a lower limit of the sizes of the scale of scattering inhomogeneities, R_{max} can be estimated [18]. This estimation is obviously limited by the resolution of the given experiment. At higher *q* values, the scattering signal decreases and falls into the background at values of *q* greater than 0.05 $Å^{-1}$. From the transition point, the geometric dimensions of the irregularities - d_{min} can be defined that correspond to the size of the smallest inhomogeneities [20]. Below this point, the scattering curves obey a power law.

As a result of alloying samarium the value of the power exponent *p* increases in As-Se-S, but decreases in As-Se-Te (Table 1.). According to the measured values, it can be argued that the addition of samarium leads to modification of the structure in the studied CGS materials in aside of a fractal nature. For As-Se-S the exponent *n* increases to 4.68, which corresponds to the diffuse scattering from the surface [21]. For the As-Se-Te samples *n* decreases to 3.85, which indicates the scattering of three-dimensional body with fractal like surfaces, $D_s = 6 - n$, where D_s is the fractal dimension of the surface, and $2 \le D_s < 3$. In our case is $D_s = 2.15$. According to [19], this behavior is characteristic to two-phase porous structures consisting of a bulk solid phase and pores, with fractal-like interfaces boundaries. [18, 22, 23].

It is considered that the lower boundary of self-similarity is determined by the size of mono disperse inhomogeneities (r_0 ~ 30 ÷ 50 Å), which constitute larger size fractal clusters (R ≈ 500 Å). The size of monodisperse heterogeneities were estimated on the basis of approximation that their dimensions may not exceed half the distance between the inhomogeneities, i.e., $r_0 = \pi/2q_{max}$ [23]. As seen from the Table 1., the doping changes the lower boundary the self-similarity in the both compositions: for $As_{33.3}Se_{33.3}S_{33.4}$ grows and for $As_{33.3}Se_{33.3}Te_{33.4}$ decreases. This effect is apparently connected with high chemical activity of sulfur, compared with tellurium.

The SANS intensity depends on the contrast ($\Delta\rho$) - the difference between the average scattering length (ρ_{ave}) of the studied particles with scattering length of the homogeneous environment. The characteristic parameter of SANS scattering curves is the $I(0)$ - scattering

intensity at zero angle. Although our data do not reach very small q values, allowing one to extrapolate to zero, nevertheless for similar types of scattering curves $I(0)$ is well correlated with their height in the measured q-range. $I(0)$ depends strongly on the contrast, the absolute value of the scattering intensity grows quadratically with $\Delta\rho$ [20]. In our samples the minor change of composition does not affect sensibly the contrast. Therefore, the observed intensity increase in As-Se-S system and decrease in the As-Se-Te by doping, is not related to the contrast change due to the composition, but rather to the strong structural changes induced by doping. Further details cannot be obtained from the present data, therefore further study is needed for elucidation of these effects. Neutron diffraction experiments on selected materials and determination of the coordination of the atoms are in progress.

Raman spectra of investigated CGS samples As_2Se_3, $As_{40}Se_{30}S_{30}$, $As_{33.3}Se_{33.3}Te_{33.4}$, $As_{33.3}Se_{33.3}S_{33.4}$, $As_{40}Se_{30}Te_{30}$, $As_{33.3}Se_{33.3}Te_{33.4}$:$Sm_{2.5}$, $As_{33.3}Se_{33.3}S_{33.4}$:$Sm_{2.5}$ are given in Fig.2.

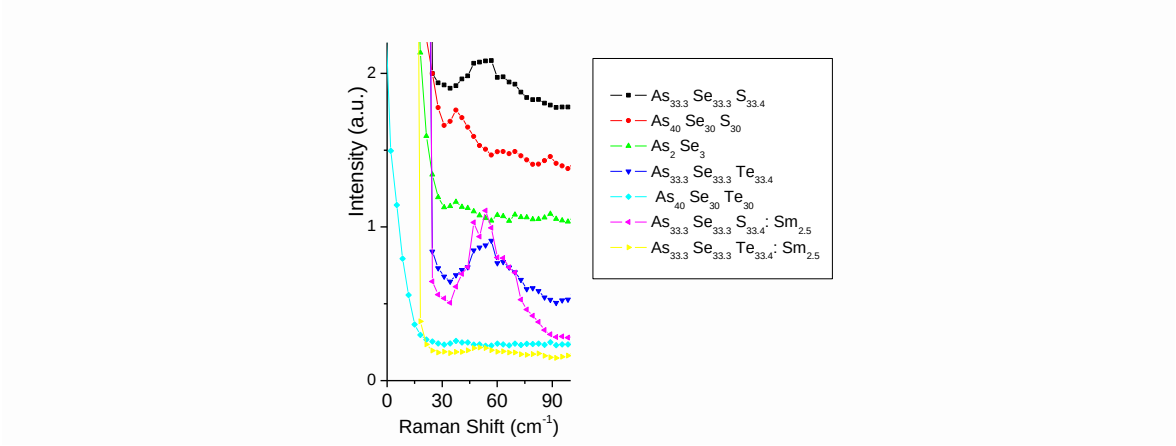

Fig. 2. Raman spectra of As_2Se_3, $As_{40}Se_{30}S_{30}$, $As_{33.3}Se_{33.3}Te_{33.4}$, $As_{33.3}Se_{33.3}S_{33.4}$, $As_{40}Se_{30}Te_{30}$, $As_{33.3}Se_{33.3}Te_{33.4}$:$Sm_{2.5}$, $As_{33.3}Se_{33.3}S_{33.4}$:$Sm_{2.5}$ chalcogenide glasses films.

It has been established that the Raman scattering (RS) of chalcogenide glass-like semiconductors (CGS) materials As_2Se_3, $As_{40}Se_{30}S_{30}$, $As_{33.3}Se_{33.3}Te_{33.4}$, $As_{33.3}Se_{33.3}S_{33.4}$, $As_{40}Se_{30}Te_{30}$, $As_{33.3}Se_{33.3}Te_{33.4}$:$Sm_{2.5}$, $As_{33.3}Se_{33.3}S_{33.4}$:$Sm_{2.5}$ at frequencies below 100 cm^{-1} consists of two parts: in the first region the intensity with increasing frequency up to 30 ÷ 40 cm^{-1} decreases (quasi-elastic scattering); in the second one - a broad band with a maximum at frequencies of ~ 63 ÷ 67 cm^{-1} is observed, usually attributed to boson peak (BP). Such behavior is not found in the studied crystals [24]. In all As_2Se_3, $As_{40}Se_{30}S_{30}$, $As_{40}Se_{30}Te_{30}$ stoichiometric compositions the BP frequencies are the same (~48.9 cm^{-1}) and significantly less than BP frequencies (67.8 cm^{-1}) of $As_{33.3}Se_{33.3}S_{33.4}$ and $As_{33.3}Se_{33.3}Te_{33.4}$ non-stoichiometric compositions. It indicates small sizes of medium order in the first case comparing with the second one. Among of the investigated stoichiometric compositions the weakest BP is observed in $As_{40}Se_{30}S_{30}$ composition. This fact is explained by high chemical activity of sulfur atoms which contributes to the creation of network-chain structure in the amorphous matrix. BP in RS spectrum of $As_{33.3}Se_{33.3}S_{33.4}$ and $As_{33.3}Se_{33.3}Te_{33.4}$ of non-stoichiometric compositions consists of several narrow maxima which overlap to a rather broad peak. It is connected with arising some molecular fragments and degrees of freedom due to chalcogenide atoms, which lead to reduction of the size of inhomogeneities and formation of new structural fragments. Of all CGS compositions the boson peak for $As_{33.3}Se_{33.3}Te_{33.4}$ has the highest intensity. It is attributed to the fact that the presence of tellurium atoms contributes to destruction of chain molecules which increases the number of broken bonds, the concentration of charged defects and degree disorder. Samarium ions affect with different nature on the local structure of materials studied. Adding samarium ions to the $As_{33.3}Se_{33.3}S_{33.4}$ composition, they interact with the material as chemically active elements and form new structural features. As a result of the chaotic orientation, ions of Sm increase the disorder. This causes increase in the intensity of the boson peak. The addition of samarium ions to the

$As_{33.3}Se_{33.3}Te_{33.4}$ composition, the intensity of the boson peak sharply decreases and vanishes. It can be explained by an increase in the degree of crystallinity and the distribution characteristics of samarium ions in the amorphous matrix. It is assumed that samarium ions are distributed in the whole amorphous matrix, which increases the degree of crystallization and decreases intensity of the boson peak.

The observed features are associated with relaxation and excess density of states of acoustic vibrations in irregularities is localized with nanometer-size of material. Such irregularity areas are associated with nano-sized inhomogeneities. Such non-homogeneous areas are observed in low-frequency Raman spectrum and also were determined by X-ray diffraction [1], in accordance with the presence of non-homogeneous regions seen by SANS. Our results show that the contribution of the different types of scattering in the low-frequency range depend on the degree of disorder in the material, which varies with the change of chemical composition and by doping.

4. Conclusions

Structural features of As-Se-S and As-Se-Te systems have been investigated on the nanometer scale. The influence of chemical composition and alloying with samarium has been characterized by densitometry, small-angle neutron and Raman scattering. It is shown that the investigated materials have two-phase porous structure, i.e. materials outfit with solid particles and include free volumes. For all samples the intensity of neutron scattering, a power law q^{-n} and such dependence continues until the values of $0.2 \div 0.4$ $Å^{-1}$, where degree factor undergoes changes, as a result of variations in the chemical composition and doping by samarium. For the $As_{33.3}Se_{33.3}S_{33.4}$ and $As_{33.3}Se_{33.3}Te_{33.4}$ the spectra obey Porod's law ($n \approx 4.12 \div 4.14$) i.e. they do not have fractal nature. Addition of samarium brings about fractal-like structural changes of the indicated compounds. In this case, the power exponent of $As_{33.3}Se_{33.3}S_{33.4}$ composition increases to value to 4.68 and for $As_{33.3}Se_{33.3}Te_{33.4}$ decreases to 3.85, in which the first case corresponds to diffuse surface, but the second corresponds to two-phase porous structure, with possibly surface fractal interfaces. It has been established that the Raman scattering (RS) of chalcogenide glass-like semiconductors (CGS) materials at frequencies below 100 cm^{-1} consists of two parts: first – at which the intensity with increasing frequency up to $30 \div 40$ cm^{-1} decreases (quasi-elastic scattering); second – in which a broad band with a maximum at frequencies of $\sim 63 \div 67$ cm^{-1} (boson peak - BP) have been observed. The addition of samarium ions to the $As_{33.3}Se_{33.3}Te_{33.4}$ composition causes a sharp decrease of the intensity of boson peak. It was explained by an increase in the degree of crystallization and the distribution characteristics of samarium ions in the amorphous matrix. It is assumed that samarium ions are distributed in the whole amorphous matrix, which increases the degree of crystallinity and decreases the intensity of boson peak.

Acknowledgments

This work has been carried out in the Budapest Neutron Centre Hungarian Academy of Sciences and was organized in the frameworks of NMI3-II-FP7 according to the grant agreement N0. 283883.

References

[1] R.I. Alekberov, S.I. Mekhtiyeva, G.A. Isayeva, et al., Chalcogenide Letters, **10**, 335 (2013).
[2] R.I. Alekberov, S.I. Mekhtiyeva, G.A. Isayeva , et al., FTP **48**, 818 (2014).
[3] R.I. Alekberov, S.I. Mekhtiyeva, G.A. Isayeva, et al., Glass Physics and Chemistry **40**, 725 (2014).
[4] R.I. Alekberov, S.I. Mekhtiyeva, G.A. Isayeva, A.I. Isayev, FTP **48**, 823 (2014).
[5] A. I. Isayev, S.I. Mekhtiyeva, R.I. Alekberov, J. Optoelectron. Adv. Mat. **18**, 39 (2016).

[6] M. Fabian, E.Svab, V. Pamukchieva, et al, Journal of Physics: Conference Series **253**, 12053 (2010).
[7] G. Yang, L. Wei, B. Bureau, et al., Phys. Rev. B **820**, 195 (2010).
[8] S. Alexander, R. Orbach, J. Physique. Lett, **43**, L625 (1982).
[9] S. Alexander, C. Laerman, R. Orbach, H. Rosenberg, Phys. Rev, **B28**, 4615 (1983).
[10] V.V. Zosimov, L.M. Lyamshev, UFN **165**, 363 (1995).
[11] É. A. Smorgonskaya, R.N. Kyutt, S.K. Gordeev, A.V. Grechinskaya, Yu. A. Kukushkina, A. M. Danishevskii, Phys. Solid State **42**, 1146 (2000).
[12] A.B. Golodenko, FTP **44**, 87 (2010).
[13] A.M. Andriesh, M.S. Iovu, and S.D. Shutov, J. Optoelectron. Adv. Mater. **4**, 631 (2002).
[14] A. Zakery, S.R. Elliott, J. Non-Cryst. Solids **330**, 1 (2003).
[15] M. Wuttig, N. Yamada, Nat. Mater. **6**, 824 (2007).
[16] A.V. Kolobov, K. Tanaka, Handbook of Advanced Electronic and Photonic Materials and Devices, ed. by H.S. Nalwa, vol. **5**. Chalcogenide Glasses and Sol-Gel Materials. Academic Press (2001) pp. 47-85.
[17] L. Rosta, Appl. Phys. A **74** (Suppl.) S52-S54 (2002).
[18] G.P. Kopitsa, V.K. Ivanov, S.V. Grigoriev, P.E. Meskin, O.S. Polezhaeva, V.M. Garamus, JETP Letters, **85**, 122 (2007).
[19] H.D. Bale, P.W. Schmidt, Phys. Rev. Lett. **38**, 596 (1984).
[20] M.V. Avdeev, V.L. Aksenov, Physics-Uspekhi, **53**, 971 (2010).
[21] Schmidt P.W., in Modern Aspects of Small Angle Scattering (Ed. H. Brumberger) Dordrecht: Kluwer Acad. Publ. (1995) p.1.
[22] B.M. Smirnov, UFN **149**, 177 (1986).
[23] V.K. Ivanov, G.P. Kopitsa, S.V. Grigoriev, O.S. Polezhaeva, V.M. Garamus, FTT **52**, 898 (2010).
[24] V.K. Malinovsky, V.N. Novikov, A.P. Sokolov UFN **163**, 119 (1993).